Chapter 4

Basic state

In contrast to the SM, the basic state of planar EHC in the WEM description is in general not trivial, i.e. $\sigma = 1$, $\phi = 0$, $\boldsymbol{n} = (1, 0, 0)$ and $\boldsymbol{v} = 0$ is not a solution of the WEM equations. For blocking electrodes this is obvious because charge conservation together with finite conductivity leads to an accumulation of charges near the electrodes. The only exception are plates having conductive properties as though the NLC would extend behind the electrodes to infinity in the z direction. Actually, this kind of "ohmic" BC is assumed in the SM. Any other BC lead to boundary layers (BL) with the general form

$$\sigma = \sigma_0(z,t) \equiv 1 + \delta\sigma_0(z,t), \quad \phi = \delta\phi_0(z,t), \quad \boldsymbol{n} = (1,0,0), \quad \boldsymbol{v} = 0. \tag{4.1}$$

Global properties of the BL can be measured. The component of the dipole momentum per area that is in phase with the external voltage leads for low frequencies to a deviation of the capacitance from its dielectric value; the component with a phase lag of $\pi/2$ leads to a contribution to the AC conductivity for low frequencies. Of course, the DC conductivity equals zero for blocking BC.

In Chapter 4.1 I formulate the problem and discuss general properties of the basic state. In the Chapters 4.2 and 4.3 the BLs arising from blocking BC are discussed in the limits of slow and fast recombination. The latter case has been investigated extensively in different contexts in the literature and I will show how the models used there are related to special cases of the WEM. Chapter 4.4 gives the current response of the NLC cell in the basic state for blocking BC in form of analytic approximations for the low-frequency behaviour of the capacitance and the conductivity. Fits to the experiments give a thickness of about 1 μm consistent with the values calculated with the WEM. It is concluded, that, at least in the I52 experiments, the BLs are not relevant for EHC. This means that, in a good approximation, the subsequent

linearization of the WEM in Chapter 5 can be carried out with respect to the trivial basic state. Thus the main part of the material contained in Chapter 5 is independent of the presentation in this chapter, and readers not interested in the problem of the basic state can continue with Chapter 5. The linear stability analysis starting from the nontrivial basic state is formulated in Appendix A.2.

4.1 Boundary layers

The investigations in this chapter are based on the general scaled WEM equations (3.18) and (3.19), without the approximations made in Chapter 3.3.1. The Eqs. (3.27) - (3.30) resulting from these approximations are the basis for the Chapters 5 and 6.

Inserting the ansatz (4.1) for the nontrivial basic state into the equations (3.18) and (3.19) results in

$$P_1 \partial_t \rho_0 = -\partial_z \left(E_0 \sigma_0\right) + D \partial_z^2 \left(2 s_1 \rho_0 + \frac{d_1 \sigma_0}{\alpha}\right), \tag{4.2}$$

$$\begin{aligned} P_1 \partial_t (\sigma_0 - \alpha d_1 \rho_0) &= -\alpha^2 s_1 \partial_z (E_0 \rho_0) + D s_1 \partial_z^2 \left(2\sigma_0 - \alpha d_1 \rho_0\right) \\ &- \frac{\tilde{r} P_1}{2} \left[\sigma_0^2 - 1 - \alpha d_1 \rho_0 - \alpha^2 s_1 \rho_0^2\right]. \end{aligned} \tag{4.3}$$

In contrast to the linearization in Chapter 5, the director relaxation plays no role, and the charge relaxation time rather than the geometric mean $\sqrt{\tau_q \tau_d}$ and the sum of the mobilities rather than their geometric mean is relevant for the basic state. Furthermore, the diffusion length in the basic state is directly related to λ_D. So I introduced as new mobility parameter the ratio of the charge relaxation time to the transition time for the mobility sum μ under the voltage V_{c0}, and as new diffusion parameter the scaled Debye length [92],

$$\alpha = \frac{\tau_q}{\tau_t} \pi^2 = \frac{\mu V_{c0} \tau_q \pi^2}{d^2} = \sqrt{\frac{P_1 \pi^2}{s_1}} \tilde{\alpha}, \tag{4.4}$$

$$D = 2 \left(\frac{\pi \lambda_D}{d}\right)^2 = \frac{\tilde{D}}{2 s_1}. \tag{4.5}$$

Assuming $\gamma = 1$, α varies from 0.016 for $T = 30°\mathrm{C}$ to 0.0032 for $T = 60°\mathrm{C}$ and $D \approx 0.01\alpha$ in the I52 experiments [31, 42]. Equations (4.2) and (4.3) are a set of partial differential equations with inhomogeneous BC for $\rho_0 = -\partial_z^2 \phi_0$ and σ_0. With respect to the z derivatives, they are of forth order in ϕ_0 and of second order in σ_0. The necessary six BC are $\phi_0(z = \pm\pi/2, t) = 0$, and the four BCs (3.24) and (3.25).

The nonlinearities arise from the recombination terms in the bracket and from the "drift advection terms" $\partial_z(E_0\rho_0)$ and $\partial_z(E_0\sigma_0)$.

A first estimate of the (scaled) BL thickness, valid for any recombination rates, is set by the amplitude λ_{mig} of the carrier-drift oscillations under the AC field, [1].

$$\lambda_{mig} = \frac{\alpha\sqrt{R}}{\pi\omega_0^{phys}\tau_q}. \tag{4.6}$$

Since the charge-density parts of the BL relax while they migrate, the effective thickness of the ρ-BL caused by the drift effects cannot exceed the distance $\lambda_q = \alpha\sqrt{R}$ travelled in one charge relaxation time.

4.2 Estimates for slow recombination

Assuming $\tau_{\rm rec} >> \tau_q$, the carrier-density mode cannot follow the oscillations of the external field, so $\sigma_0(z)$ is assumed to be approximately constant in time. The blocking BC induce oscillating charges, so $\rho_0(z,t)$ oscillates with the external field. We are only interested whether there are boundary layers that are much thicker than the ρ-BL whose thickness is bounded by λ_{mig}, Eq. (4.6). Outside the ρ-BL, the Eqs. (4.2) and (4.3) can be linearized. The ansatz

$$\begin{aligned} \rho_0 &= (\rho_0^+ \cos\omega_0 t + \rho_0^- \sin\omega_0 t)e^{-k(z-\pi/2)}, \\ \delta\sigma_0 &= \sigma_0^0 e^{-k(z-\pi/2)} \end{aligned} \tag{4.7}$$

leads to three eigenvalues k_n corresponding to three characteristic lengths $\lambda_{\rm BL,n} = 1/k_n$. There are two modes dominated by ρ with $\lambda_{\rm BL}$ of the order of λ_D, and much less than λ_D, respectively. The third mode dominated by σ has the decay length

$$\lambda_{BL,\sigma} = \sqrt{\frac{s_1(R\alpha^2 + 2D)}{\tilde{r}P_1}}. \tag{4.8}$$

For a zero electric field, the three modes are decoupled and $\lambda_{BL,\sigma}$ results from the interplay of diffusion and recombination relaxation of the σ field. For $\tilde{r} = 0.05$ relevant for an experiment using I52 (see Chapter 5.5), the thickness of the σ-BL would be nearly 40% of the cell thickness, but this mode is not excited for blocking BC. Nevertheless, this problem should be investigated numerically.

[1] In this estimate, $2\sqrt{2}/\pi$ is set equal to one.

4.3 Limit of fast recombination

If $\tau_{\rm rec} << \omega_0^{-1}$ and $\tau_{\rm rec} << \tau_d$, the carriers are in local equilibrium with respect to the dissociation-recombination reaction so that $n^+n^- = n_0^2$. This corresponds to $\tilde{r} \to \infty$, i.e., the bracket in Eq. (4.3) must become zero. This is automatically fulfilled by expressing the carrier densities in terms of the "diffusion potential" u, defined by $n^\pm = n_0 e^{\pm u}$, or

$$\rho_0(u) = \frac{2\sinh u}{\alpha}, \tag{4.9}$$

$$\sigma_0(u) = \frac{e^u + \gamma e^{-u}}{1+\gamma}. \tag{4.10}$$

The right-hand side of (4.2) becomes $-\partial_z J_0$ where the current is given by

$$J_0(u) = \sigma_0(u)\left[E_0 - \frac{D}{\alpha}\partial_z u\right] = \sigma_0(u)\left[E_0 - \frac{V_T}{V_{c0}}\partial_z u\right], \tag{4.11}$$

and Eq. (4.2) itself can be written as

$$P_1 \partial_t \sinh u = -\sigma_0(u)\left[\frac{\alpha}{2}\ \frac{J_0(u)\partial_z\sigma_0(u)}{\sigma_0^2(u)} + \sinh u - \frac{D}{2}\partial_z^2 u\right]. \tag{4.12}$$

The form of the current is obvious from the derivation of the WEM. In the fast-recombination limit, the thermodynamic forces $\boldsymbol{F}^\pm$, Eqs. (3.6), are given by $\boldsymbol{F}^\pm = \mp e\boldsymbol{\nabla}(\tilde{\phi}_0 + V_T u)$, so $J_0 = \mu_\perp^+ \partial_z F_z^+ - \mu_\perp^- \partial_z F_z^- = \sigma_\perp \partial_z (E_0 - V_T \partial_z u)$, which is just Eq. (4.11) in physical units.

The electric field in the Eqs. (4.11) and (4.12) is given by

$$E_0(z,t) = E_b(t) + \int_{-\pi/2}^{z} dz \rho_0(u) \tag{4.13}$$

where the field $E_b(t) = E_0(z = -\pi/2)$ is determined by the condition $J_0(u) = 0$ at $z = -\pi/2$ with J_0 from Eq. (4.11). After some transformations using the condition of overall neutrality $E_0(z = -\pi/2) = E_0(z = \pi/2)$, the result is

$$E_b(t) = \frac{1}{\pi}\left(p(t) - \sqrt{2R}\cos\omega_0 t\right), \tag{4.14}$$

$$p(t) = \int_{\pi/2}^{\pi/2} dz z \rho_0 = 2\int_{\pi/2}^{\pi/2} dz z \frac{\sinh u}{\alpha}. \tag{4.15}$$

$p(t)$ has the physical meaning of a dipole momentum per area.

Equation (4.12) with (4.11), (4.9) and (4.10) represents a partial integro-differential equation for the field $u(z,t)$. The "integro" part comes from the electric field, Eq. (4.13) and the BC (4.14). It was solved numerically with a finite-difference method in real space. The z derivatives are represented as centered differences of second order and the integral parts are calculated using the trapezoid rule. For the time steps, an implicit second-order Crank-Nicholson method was applied for all local terms and an Euler step for the nonlocal parts. For the numerical calculations [93], space was scaled by λ_D, time by τ_q and the voltage by V_T, and then the equations (4.12) and (4.14) take the compact form ($u' \equiv \partial_z u$)

$$\partial_t \sinh u = -\sigma_0(u)[\sinh u - u''] + \left[u' - u'_b - \int_0^z dz \sinh u\right] \frac{\partial \sigma_0}{\partial u} u', \quad (4.16)$$

$$u'_b = \frac{\lambda_D}{d}\left[\int_{-d/2\lambda_D}^{d/2\lambda_D} dz z \sinh u - \frac{\overline{V}\sqrt{2}}{V_T} \cos \omega_0^{phys} \tau_q t\right]. \quad (4.17)$$

Note that in this scaling the integro-PDE itself contains only the ratio γ while the BC (4.17) contains the three system parameters of the basic state, $\frac{d}{\lambda_D}$, $\frac{\overline{V}}{V_T}$ and $\omega_0^{phys}\tau_q$. The BCs are implemented by calculating from (4.17) two "virtual" points just one grid unit outside of either electrode and using these points in the z derivatives of the next step. As initial conditions, all fields were set equal to zero and several external periods (typically 10 corresponding to 10^4 time steps) were simulated before the actual period which is plotted to obtain approximately steady-state conditions.

In the following, I present results for $\gamma = 1$. In this case, further simplifications are possible (see below), which are not essential for the numerical solution, but can be used to make contact with previous work.

Figure 4.1 (a) shows the field $u(z,t)$ and Figure 4.1 (b) the electric field $E_0(z,t)$ in the WEM scaling for the parameters $d/\lambda_D = 26$, $\overline{V}/V_T = 143$, and $\omega_0^{phys}\tau_q = 0.2\pi$. Figure 4.2 shows $u(z,t)$, $E_0(z,t)$, and the local current density $I_0(z,t)$, for a higher frequency of the AC voltage. In physical units, the voltage is half of the threshold voltage in the MBBA experiments [39, 40]. The thickness of 13μm in these experiments corresponds to $\lambda_D = 0.5\ \mu$m or, with the formula for λ_D in Table 3.2 and for $\sigma_\perp = 10^{-8}(\Omega\text{m})^{-1}$, to $\mu = 3 \times 10^{-9}\text{m}^2/(\text{Vs})$.

Since in a rather large part of the bulk region the fields are nearly those of the trivial SM state, the electric field in units of V_T/λ_D, rather than the voltage, determines the dynamics of the BLs. The spatio-temporal behaviour of the scaled fields in the Figs. 4.1, 4.2, and Fig. 4.3 is invariant under a transformation $\overline{V} \to \beta\overline{V}'$, $\lambda_D \to \beta^{-1}\lambda'_D$ corresponding to $\mu \to \beta^{-2}\mu'$.

Figure 4.3 illustrates how the blocking BCs lead to a charge accumulation. In

Figure 4.1 (a) Diffusion potential u = $\ln(n^+/n^-)$ and (b) local electric field, $\boldsymbol{E} = E_0\hat{\boldsymbol{z}}$ of the WEM basic state in the fast-recombination limit for blocking electrodes and for an applied voltage corresponding to half of the threshold voltage. Assumed is an Debye length of $\lambda_D = 0.5\ \mu$m .

Figure 4.2 (a) Diffusion potential, (b) local electric field, and (c) local current for the MBBA cell of Fig. 4.1 above, but for a higher external frequency of $\omega_0 \tau_q = \pi$.

contrast to strongly injecting electrodes which can lead to the Felici instability [82], the blocking BC lead to a volume force which points always towards the electrodes and thus acts stabilizing.

Note that, in principle, Equation (4.12) can be written as a PDE of third-order with respect to the z derivatives by solving for E_0, differentiating both sides, and setting $\partial_z E_0 = \rho_0 = 2\sinh u/\alpha$. This form is, however, numerically less stable.

Special cases

For equal mobilities ($\gamma = 1$), the condition $n^+n^- = n_0^2$ can be written as $\sigma_0 = (1+\tilde{\rho}_0^2)^{1/2}$ and (4.2) becomes

$$P_1 \partial_t \tilde{\rho}_0 = -\tilde{\rho}_0 \sqrt{1+\tilde{\rho}_0^2} - \frac{\alpha E_0 \tilde{\rho}_0}{2\sqrt{1+\tilde{\rho}_0^2}} \partial_z \tilde{\rho}_0 + \frac{D}{2} \partial_z^2 \tilde{\rho}_0. \tag{4.18}$$

The three terms on the right-hand side can be interpreted as relaxation of the charges with the linear relaxation rate enhanced by a factor of $(1+\tilde{\rho}_0^2)^{1/2}$, while the carriers drift with the velocity $\mu^+ E_0$ of either species times a factor $\tilde{\rho}_0/(1+\tilde{\rho}_0^2)^{1/2}$, and diffuse with a constant rate. The slowing down of the effective velocity for decreasing $\tilde{\rho}_0^2$ is illustrated by the "charge wave" in Fig. 4.2 for t=0...π near the left electrode and in Figure 4.3, where the charge wave moves quickly to the right if $\tilde{\rho}_0^2$ is large (Figures 4.3a - 4.3c) and slows down and eventually relaxes (Figures 4.3d and 4.3e).

In the stationary case (DC driving), charge conservation implies a constant current and Eq. (4.12) reduces to the condition that the bracket be zero. Neglecting diffusivities, this condition can be writen as

$$du \left(\frac{e^u - \gamma e^{-u}}{(e^u + \gamma e^{-u})^2 (e^u - e^{-u})} \right) = -\frac{dz}{J_0 \alpha (1+\gamma)}. \tag{4.19}$$

The integration gives the rather lengthy Eq. (14) in Ref. [81]. In the unipolar limit this gives the well-known basic state $\rho_0 = (J_0/(2\alpha)^{1/2}$ of the Felici instability [82].

At last, the linearization of (4.12) in the stationary limit ($E_0 = \sqrt{R}/\pi$) gives two decay length scales associated with the combined effects of diffusion, drift and relaxation.

4.4 Low-frequency behaviour of the resistance and the capacitance

Throughout this section I use unscaled (physical) units. The general current response for any BC is the sum of the conductivity current and the displacement current. For

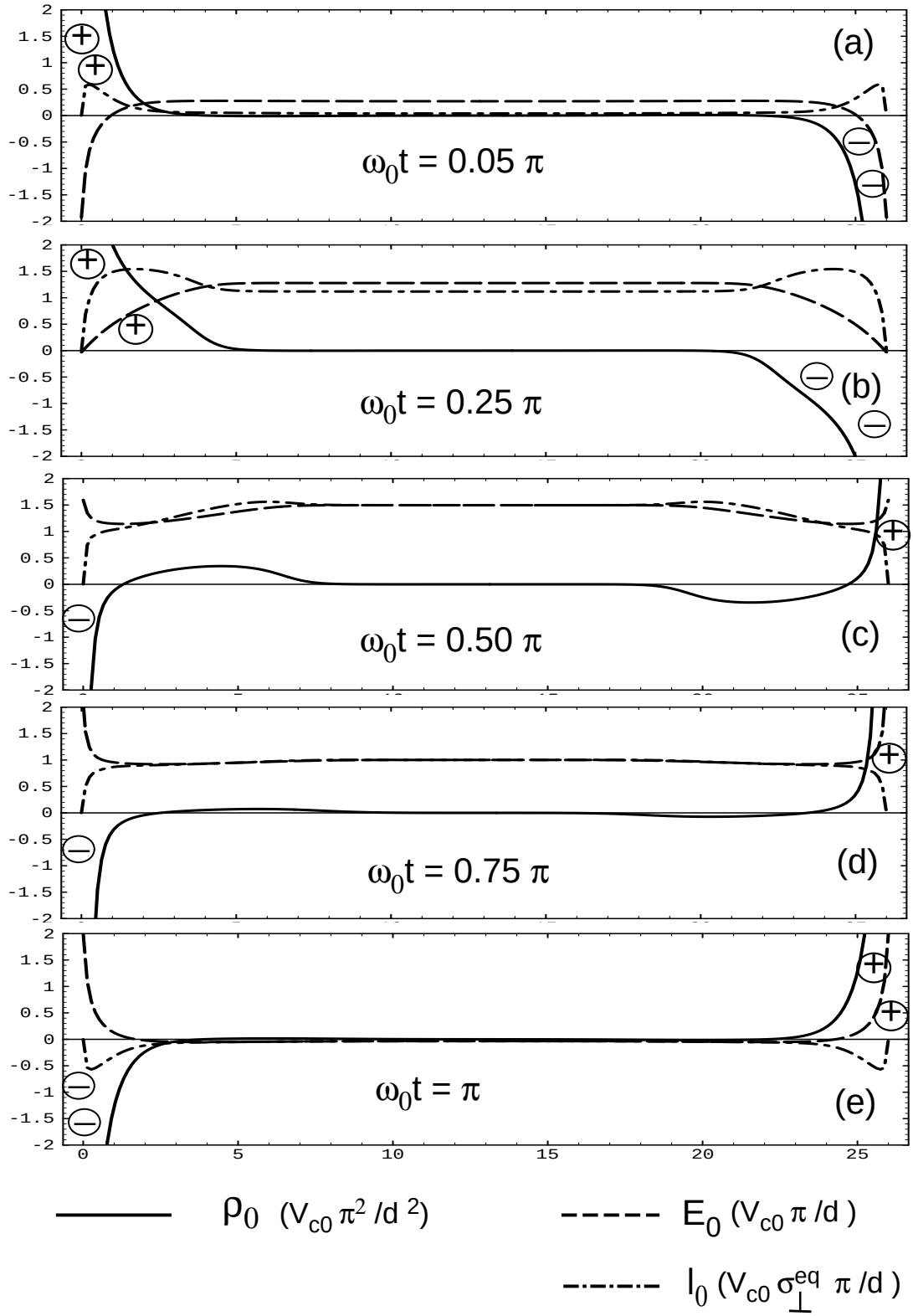

Figure 4.3 Snapshots of the WEM basic state of Fig. 4.1 for five times covering a half period. Shown is the space charge $\tilde{\rho}_0 = \sinh u$ (solid), the local field E_0 (dashed), and the local current I_0 (point-dashed).

a NLC cell with an area A in the x and y directions, one obtains

$$I(t) = A\left[j_z + \partial_t \epsilon_0 \left(\underline{\underline{\epsilon}}\boldsymbol{E}\right)_z\right], \tag{4.20}$$

where $\boldsymbol{j}$ and $\partial_t \epsilon_0 \underline{\underline{\epsilon}}\boldsymbol{E}$ are the conductivity and displacement currents. With the help of charge conservation, Eq. (4.20) can be transformed into

$$I(t) = A\left[\overline{j}_{BC} + \partial_t\left(\epsilon_0 \overline{\epsilon_{3j} E_j} + \frac{p(t)}{d}\right)\right], \tag{4.21}$$

where $\overline{x}$ denotes the average of the quantity x over the cell volume and $\overline{j}_{BC}$ is the horizontally averaged current density through the boundaries ($\overline{j}_{BC} = 0$ for blocking BC). Overall neutrality implies $\overline{j}_{BC}(z = -d/2) = \overline{j}_{BC}(z = +d/2)$.

Below threshold, the averaged displacement current $\epsilon_0 \partial_t \overline{\epsilon_{3j} E_j} = \epsilon_0 \epsilon_\perp \partial_t V(t)/d$ is strictly in phase with the time derivative of the voltage and leads to the dielectric capacitance. For blocking BC, all nontrivial parts of the resistance and the capacitance are related to $p(t)$.

4.4.1 AC Resistance and capacitance

The AC resistance R [2] and capacitance C are defined by the Fourier-transformed current response $I(\omega)$,

$$\frac{1}{R} = \mathrm{Re}\frac{I(\omega)}{V(\omega)}, \tag{4.22}$$

$$C = \frac{1}{\omega}\mathrm{Im}\frac{I(\omega)}{V(\omega)}. \tag{4.23}$$

With Eq. (4.21), one arrives at

$$\frac{1}{R} = \frac{A}{d}\left[-\omega \mathrm{Im}\left(\frac{p(\omega)}{V(\omega)}\right) + \mathrm{Re}\left(\frac{\overline{j}_{BC}(\omega) d}{V(\omega)}\right)\right], \tag{4.24}$$

$$C = C_{diel} + \frac{A}{d}\left[\mathrm{Re}\left(\frac{p(\omega)}{V(\omega)}\right) + \frac{1}{\omega}\mathrm{Im}\left(\frac{\overline{j}_{BC}(\omega) d}{V(\omega)}\right)\right], \tag{4.25}$$

where $C_{diel} = A\epsilon_0\epsilon_\perp/d$.

[2] In this section, R is not the control parameter

4.4.2 Analytic approximations for blocking boundaries

The considerations in the previous sections show, that in a good approximation $\lambda_{\rm BL} << 1$ for the relevant modes. In addition, I assume for the BLs the functional form

$$\rho_0 = \rho_l(t)e^{-(z-d/2)/\lambda_{BL}} + \rho_r(t)e^{-(d/2-z)/\lambda_{BL}}, \quad \rho_l = -\rho_r. \tag{4.26}$$

(in view of, e.g., Figure 4.1, this is a rather crude approximation). Charge conservation leads to a dynamical equation for ρ_l which can be expressed as one for the dipole moment per area,

$$\partial_t p = -\frac{2\lambda_{BL}}{\tau_q d}p + V(t)\sigma_\perp. \tag{4.27}$$

Substituting this into (4.24) and (4.25) yields the result

$$R = R_\infty \left(1 + \left(\frac{\lambda'}{\omega_0\tau_q}\right)^2\right), \tag{4.28}$$

$$C = C_{diel}\left(1 + \frac{\lambda'}{(\omega_0\tau_q)^2 + \lambda'^2}\right), \tag{4.29}$$

where $R_\infty = d/(A\sigma_\perp)$ is the high-frequency resistance and $\lambda' = 2\lambda_{\rm BL}/d$ is the fraction of the cell volume occupied by the BLs.

Fitting these relations to the capacitance and resistivity measurements of Dennin [31] gives an effective thickness of the charge BL of about 0.9 μm . In the experiments, the external frequency always satisfies $\omega_0^{phys}\tau_q >> \lambda'$, so Eq. (4.29) predicts $C - C_{diel} \approx \lambda'/(\omega_0^{phys}\tau_q)^2$. The measured low-frequency behaviour, however, fits better to a $(\omega_0^{phys}\tau_q)^{-1}$ law. The discrepancy is possibly a result of the the crude approximation (4.26).